Available online at www.sciencedirect.com
SCIENCE DIRECT
Biochimica et Biophysica Acta 1757 (2006) 262–272
BIOCHIMICA ET BIOPHYSICA ACTA
BBA
http://www.elsevier.com/locate/bba

Mitochondrial dysfunction in patients with severe sepsis: An EPR interrogation of individual respiratory chain components

Dimitri A. Svistunenko [a], Nathan Davies [a,1], David Brealey [b], Mervyn Singer [b], Chris E. Cooper [b,*]

[a] Department of Biological Sciences, University of Essex, Wivenhoe Park, Colchester, Essex CO4 3SQ, UK
[b] Department of Medicine and Wolfson Institute of Biomedical Research, University College London, London W1T 3AA, UK

Received 12 October 2005; received in revised form 14 February 2006; accepted 3 March 2006
Available online 30 March 2006

Abstract

Electron paramagnetic resonance (EPR) spectra of complex biological systems contain information about the paramagnetic centres present. Retrieving such information is important since paramagnetic species are common intermediates of all redox reactions in both normal and abnormal metabolism. However, it is often difficult to determine the nature and content of all paramagnetic species present because the EPR signals from individual centres overlap. Here, we apply our deconvolution method based on spectra subtraction with variable coefficient to quantify individual paramagnetic components of human muscle biopsies taken from critically ill patients with severe sepsis. We use low temperature EPR spectroscopy to identify and quantify nine different paramagnetic species in the tissue. These include the majority of the mitochondrial iron–sulfur centres and the first in vivo report of a mitochondrial radical assigned to a spin-coupled pair of semiquinones ($SQ^{\bullet}$–$SQ^{\bullet}$). We have previously demonstrated in these same muscle biopsies that biochemical assays of mitochondrial dysfunction correlate with clinical outcomes (D. Brealey, M. Brand, I. Hargreaves, S. Heales, J. Land, R. Smolenski, N.A. Davies, C.E. Cooper, M. Singer, Association between mitochondrial dysfunction and severity and outcome of septic shock. Lancet 360 (2002) 219–223.). Analysis of the paramagnetic centres in the muscle confirms and extends these findings: the ($SQ^{\bullet}$–$SQ^{\bullet}$) radical species negatively correlates with the illness severity of the patient (APACHE II score) and a decreased concentration of mitochondrial Complex I iron–sulfur redox centres is linked to mortality.

Keywords: Mitochondria; EPR; Free radical; Sepsis; Iron sulfur; Complex I; Muscle

1. Introduction

Electron transfer in redox reactions plays a fundamental role in biochemistry. The intermediates of such reactions contain an odd number of electrons and therefore have a non-zero total electron spin. Such molecular states are called paramagnetic and can be detected by the method of electron paramagnetic resonance (EPR) spectroscopy. The paramagnetic intermediates of redox reactions are usually transient, short-lived species. However, a steady state concentration of such species can be frequently detected in normally functioning complex biological systems such as cell cultures or whole tissues. For example, the process of haemoglobin (Hb) autoxidation in normal human blood results in a continuous generation (and decay) of a globin free radical [1,2], shown to be located on a tyrosine residue [3]. On the other hand, a biochemical system can be brought to a fully reduced or fully oxidised state in which not a steady state, but rather a fixed concentration of paramagnetic centres can be detected by EPR. Mitochondrial electron transfer proteins can be assayed under either equilibrium or steady state conditions [4,5]. These electron transfer proteins contain iron–sulfur clusters of two, three or four iron atoms; depending on the combination of the Fe^{3+} and Fe^{2+} oxidation states of the iron atoms in these clusters, the whole protein may be paramagnetic (EPR visible) [5].

Biological samples usually contain many different types of paramagnetic centres. Their EPR signals overlap and make

Abbreviations: APACHE II, acute physiology and chronic health evaluation (score); EPR, electron paramagnetic resonance; FMN, flavin mononucleotide; Hb, haemoglobin; h.s., high spin; l.s., low spin; Mb, myoglobin; TTFA, thenoyltrifluoroacetone

* Corresponding author. Tel.: +44 1206 872752; fax: +44 1206 872592.
E-mail address: ccooper@essex.ac.uk (C.E. Cooper).
[1] Present Address: University College London, Institute of Hepatology, 69–75 Chenies Mews, London WC1E 6HX, UK.

0005-2728/$ - see front matter © 2006 Elsevier B.V. All rights reserved.
doi:10.1016/j.bbabio.2006.03.007

analysis difficult, sometimes impossible. Although a significant number of EPR studies have been performed on animal [6–15] and human [1,2,16–20] tissues and bacteria, conventional techniques of EPR spectroscopy do not allow for the accurate characterisation (and quantitation) of individual paramagnetic species with overlapping EPR signals in complex systems. Overlapping EPR signals must be deconvoluted into components before an assignment of the signals to individual paramagnetic centres can be performed. We have previously suggested a technique of spectra subtraction with variable coefficient that has proved effective in studying individual paramagnetic centres [3,21–26]. The purpose of this communication is to demonstrate how this technique can be applied to as complex a system as whole muscle tissue in order to quantitate all paramagnetic species detectable. We will consider the low temperature spectra of whole blood and muscle biopsies of patients with sepsis, focussing on the latter as muscle bioenergetic properties have been reported abnormal. Our studies reveal changes in mitochondrial signals in the pathophysiological state, only some of which were predictable from our previous in vitro assays of enzyme activity.

2. Materials and methods

2.1. Patients

Approval for this study was obtained from the ethics committee of the University College London Hospitals National Health Service Trust. Patients (or their next-of-kin) were asked for informed consent (or agreement) before enrolment. Data were obtained from 26 patients. Full details of the patient groups and procedures for obtaining biopsies have been reported elsewhere [27]. Briefly, patients with recent-onset severe sepsis or septic shock were studied within 24 h of admission to the intensive care unit at University College London Hospitals NHS Trust. Illness severity of each patient was measured by the Acute Physiology and Chronic Health Evaluation (APACHE II) Score [28]. Tissue biopsies (approximately 200 mg) were taken from the *vastus lateralis* thigh muscle. A control group consisted of nine otherwise healthy patients undergoing elective total hip replacement for degenerative arthropathy.

2.2. Tissue sample preparation

The tissue samples were placed in both-end-open Wilmad SQ EPR tubes (Wilmad Glass, Buena, NJ) which were then frozen in liquid nitrogen. To minimize the effect that slightly different size of the tubes might have on the quantitative results, only selected tubes were used with outer diameter 4.05±0.07 mm and inner diameter 3.12±0.04 mm (mean±range). The tubes were filled with tissue samples tightly (avoiding the formation of air spaces) to a depth greater than the working zone of the resonator (1.3 cm). This meant that for tubes of equal diameter, the amount of tissue that generated the EPR spectrum was always the same.

2.3. Reduction of tissue samples with dithionite

Frozen tissue samples were pushed out of the EPR tube, weighed and placed in 450 μl of 75 mM phosphate buffer (pH 7.4) to thaw. Once thawed, the sample was homogenised with a Kinematica AG (Luzernerstrasse 147a, CH-6014 Littau-Lucerne, Switzerland) handheld homogeniser Polytron PT 1200 CL (5 s at maximal speed). A volume of 92 μl of dithionite stock solution (160 mM) was added to the homogenate and the mixture incubated at 4 °C for 3 min. The reduced homogenate was then placed into the same EPR tube (washed and dried) with a syringe attached to the other end of the tube; the tube was then incubated in liquid nitrogen vapour until frozen (~1 min) and then placed into liquid nitrogen (direct immersing into liquid nitrogen, without pre-incubation in the vapours, could result in tube cracking). The tissue samples were homogenised and reduced in turn, so a fresh dithionite stock solution was prepared for every five consecutively thawed, homogenised and reduced tissue samples. The final concentration of dithionite was about 20 mM, slightly varying according to individual dilution factors. The final dilution factor for the tissue components was also determined individually, depending on the initial tissue sample weight (the range was 150–230 mg; 1 mg was considered equivalent to 1 ml).

2.4. EPR spectroscopy

All EPR spectra were measured on a Bruker EMX EPR spectrometer (X-band) equipped with a spherical high quality Bruker resonator SP9703 and with an Oxford Instruments liquid helium system for EPR measurements at low temperature. EPR spectra simulations were performed with WINEPR SimFonia 1.25 (Bruker Spectrospin Ltd., Coventry, UK).

2.5. EPR spectra subtraction with variable coefficient

Fig. 1 shows an illustrative example of how the technique of spectral subtraction with variable coefficient can be used. The EPR spectra A and B are both sums of different EPR signals; importantly, the partial proportion of these signals is different in the two spectra: the intensity of the signal that causes the trough at the *g*-factor value of 1.99 (we shall call it EPR signal X) is notably greater in spectrum A. A difference spectrum B–kA is constructed, and the coefficient k is varied until the EPR signal at $g=1.99$ completely disappears from the difference spectrum. This happens at $k=0.42$, when a smooth baseline is observed in the difference spectrum (formally k is varied until the second derivative of the difference spectrum does not cross zero in the region of the signal's width). Signal X, responsible for the $g=1.99$ feature, may have other components, not as clearly manifested as the 1.99 line. But all those components (if any) will be changing simultaneously with k, so the difference spectrum at $k=0.42$ does not have signal X at all. If the intensity of signal X in spectrum A is taken to be 1, then the intensity of the signal in spectrum B is 0.42. Spectrum A

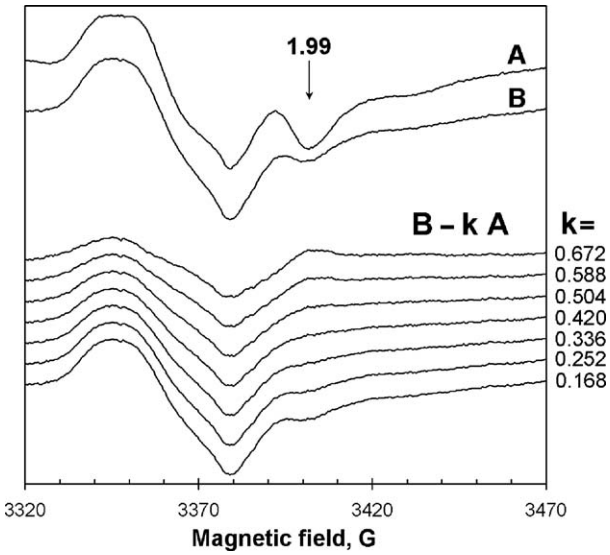

Fig. 1. An illustration of the procedure of spectra subtraction with variable coefficient This can be used first to eliminate an EPR signal from the overall EPR spectrum and then to determine the signal's intensity in relative units. The experimental spectra A and B in this example are those of muscle tissue biopsies taken from two patients with sepsis. The difference spectrum at $k=0.42$ does not contain the $g=1.99$ signal. Instrumental conditions: microwave power $P=3.18$ mW; microwave frequency $\nu=9.47$ GHz; modulation amplitude $A_m=3$ G; modulation frequency $\nu_m=100$ kHz; time constant $\tau=41$ ms; sweep rate v=5.96 G/s; number of scans averaged (NS)=8; registration temperature $T=10$ K.

can be used in the same way to determine the intensity of signal X (in relative units) in a series of spectra. To convert signal X intensity in a series of spectra to absolute concentrations of the paramagnetic species responsible for signal X, we would need a pure EPR lineshape of signal X, which should be double integrated, and the integral should be compared with a double integral of an EPR spectrum of a concentration standard (often Cu^{2+} ions in solution).

2.6. Normalisation of derived data

In order to correct for differences in mitochondrial density in the sample collected, all muscle spectra were initially normalised to citrate synthase activity (a mitochondrial marker enzyme) measured as described previously [27]. The intensity of individual EPR signals was then compared to the average intensity of that signal in the control samples ($n=9$). For illustrative purposes and because it does not affect the statistical analysis, in the figure showing the mortality outcome (Fig. 9), the data for the paramagnetic components in the patients who died is normalised to the mean value of the same components in the group that survived (the latter normalised to 1 for every species).

3. Results and discussion

3.1. EPR spectra of human blood and muscle

Fig. 2 shows the X-band (9 GHz) EPR spectra of human venous blood and muscle measured at a low temperature. The most pronounced feature in both spectra is the signal at $g=5.9$ originating from haem proteins in the high spin (h.s.) ferric (Fe^{III}) state [29]. In blood, this EPR signal is associated with methaemoglobin (metHb) [1]. The peak at $g=5.85$ is the perpendicular component of the axially symmetrical spectrum of the h.s. metHb, whereas the parallel component is detected at a much higher magnetic field giving the g-factor value of 2.00 [29]. Oxidised haem proteins can exist also in the low spin (l.s.) state, when the 6th coordination position of the haem ferric ion is occupied by a small molecule or by a side group of an amino acid residue [30]. Normally, there is a number of different l.s. forms of metHb in blood, formed by different ligands at the distal (6th) coordination site [22]. Their relative and absolute concentrations depend on a number of factors and are variable in different individuals and even in the samples taken from the same individual at different time. Spectrum A in Fig. 2, being an arithmetic sum of the spectra of the samples from four different patients, shows a low concentration of the l.s. forms of metHb. One of those, just detectable at $g_1=2.59$ $g_2=2.18$ and $g_3=1.83$, can be identified as hydroxyl haemoglobin (where the distal ligand is hydroxyl anion OH^-) [30].

Catalase is another haem protein that can be detected in whole blood. Its resting ferric state has the haem in the h.s. form but, in contrast to the h.s. form of metHb, the geometry of the haem is distorted and does not show an axial symmetry (the porphyrin ring is slightly stretched). As a result, the two components, that have equal g-factors and are therefore 'perpendicular' in the case of axial symmetry ($g=5.85$ in metHb), are split into $g_1=6.49$ and $g_2=5.31$, and the third component (the parallel $g=2.00$ component in metHb) is shifted to a higher field to the value of $g_3=1.98$ (Fig. 2) [8].

The EPR signal in the blood spectrum with a g-factor of 4.28 is characteristic of non-haem h.s. ferric ions Fe^{III} in rhombic coordination [31]. The specific lineshape of this signal (Fig. 2A) is a signature of the bicarbonate ions (HCO_3^-) participating in such coordination [32]. The plasma protein transferrin, that binds iron in a bicarbonate-dependent mode, is responsible for this EPR signal in blood [32].

The $g=2.05$ EPR signal in the blood spectrum (Fig. 2A) is a typical signal of copper ions in the oxidised state Cu^{2+} [33]. The interaction of the copper nucleus with a spin of $I=3/2$ with the unpaired electron results in a hyperfine splitting into four lines. This is usually seen well for the parallel component of the

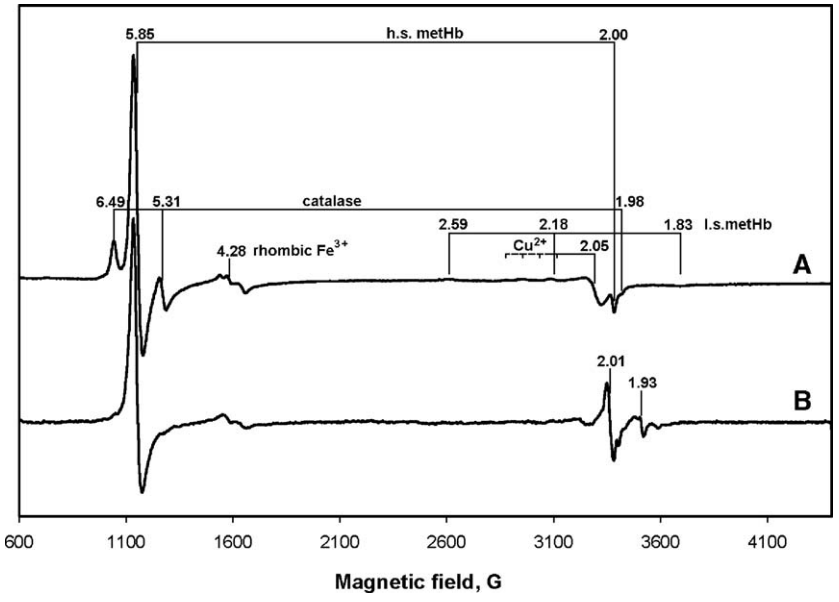

Fig. 2. The EPR spectra of blood (A) and muscle (B) from patients with severe sepsis. Each spectrum is an average of 4 individual spectra taken from different patients. The g-factors of major EPR centres are indicated. The instrumental conditions were (see Fig. 1 legend for letter coding): $P=3.18$ mW; $\nu=9.467$ GHz, $A_m=5.0$ G; $\nu_m=100$ kHz; $\tau=82$ ms; v=22.64 G/s; NS=1; $T=10$ K.

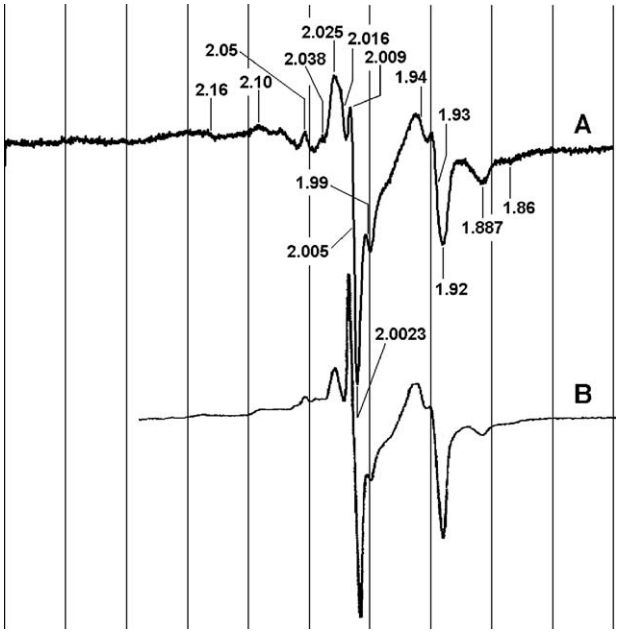

Fig. 3. The EPR spectrum of muscle in patients with severe sepsis (A) and the spectrum of tightly coupled activated bovine heart submitochondrial particles during steady-state NADH oxidation [36] (B). Since the spectra were measured at different microwave frequencies, their resonance field values are also different and therefore omitted. Instead, the spectra were overlaid on the basis of common g-factor and gridlines were drawn at an interval of 100 G. The g-factors of major features in the spectrum of tissue are indicated. The instrumental conditions for A were (see Fig. 1 legend for letter coding): P=0.05 mW; ν=9.470 GHz, A_m=3.0 G; ν_m=100 kHz; τ=41 ms; v=9.56 G/s; T=10 K. The spectra of samples from 11 patients, each sample recorded at NS=4, were averaged to produce spectrum A. Spectrum B was measure at P=2 mW and T=16 K [36].

spectrum on the left from the main perpendicular feature, but often unresolved for the latter. The centre mostly (though maybe not exclusively) responsible for this signal in blood is ceruloplasmin, the blue multi-copper oxidase present in plasma [34].

The last EPR signal that can be seen in the EPR spectrum of whole blood is the small singlet at g=2.004 from free radicals. This signal is not indicated in Fig. 2 since it overlaps with the parallel component of the h.s. metHb at g=2.00. The free radicals responsible for this signal are tyrosyl radicals formed on haemoglobin following its interaction with peroxide; the nature of these radicals has been described in details elsewhere [1–3].

Once all EPR signals in blood spectra are identified, the relative concentration of the paramagnetic centres responsible for them can be directly determined by using the technique of spectra subtraction with variable coefficient, as explained in Fig. 1 and in the text above.

The muscle spectrum B in Fig. 2, as well as blood spectrum A, has a strong signal from h.s. ferric haem proteins in the g=6 region. This spectrum originates from the muscle tissue protein myoglobin in the oxidised (met) form (metMb) and from methaemoglobin (metHb). We think that metMb is likely to be the dominant component as the g=6 signal is significantly smaller in tissues containing no myoglobin, e.g., liver [35]. Traces of the h.s. catalase EPR signal can be seen at both sides from the g=6 signal. A signal from rhombic ferric iron at g=4.3 is also present, though its lineshape is different from that in blood; it is probable that a number of species contribute to this signal. The area of the spectrum covering the magnetic field range of 2800–3800 G contains many overlapping EPR signals. The analysis of this area, i.e., deconvolution of the spectrum to composite components, assignment of each component to a paramagnetic centre and quantitation of all centres (concentration determination), would make the paramagnetic description of human muscle tissue complete.

3.2. EPR spectra deconvolution and assignment of each individual species

The EPR spectrum of human muscle shown in Fig. 3A covers a 1000 G wide area around the g-factor value of 2. It is obvious that many paramagnetic centres with different EPR signals contribute to this spectrum. Most of these centres are in mitochondria of the muscle tissue, as can be concluded from the comparison of spectrum (A) with the spectrum of purified and concentrated submitochondrial particles (Fig. 3B). The latter spectrum has been taken from the literature [36].

Mitochondria contain the respiratory chain (Fig. 4), a set of protein complexes associated with the inner membrane and participating in the transfer of electrons from the substrates (NADH and succinate) to molecular oxygen. Depending on the substrate-to-oxygen ratio, the whole chain, or a part of it, could be either reduced or oxidised, and, depending on the combination of the oxidation states Fe^{3+} and Fe^{2+} in the multinuclear

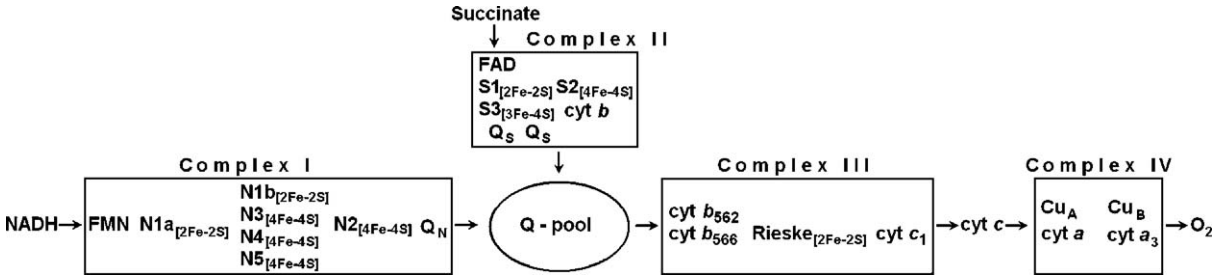

Fig. 4. Schematic presentation of the respiratory chain redox components in the inner membrane of mammalian mitochondria (after Ohnishi [36]). Iron–sulfur clusters in the NADH–ubiquinone (Complex I) and succinate–ubiquinone (Complex II) oxidoreductase segments are indicated by symbols N and S, respectively. The numbers of iron and sulfur atoms involved in each cluster are indicated by the subscripts. The Complex I components are arranged in the box by their redox midpoint potential increasing from the left (FMN, flavin mononucleotide) to the right (N2).

Table 1
The *g*-factors of the iron–sulfur clusters

Fe–S cluster	g_x	g_y	g_z	Reference
N1a	Not visible			[36]
N1b	2.022	1.938	1.923	[53]
N3	2.037	~1.93	1.86–1.87	[54,55]
N4	2.10–2.11	~1.94	1.88	[54]
N5	2.07	1.93	1.90	[36]
N2	2.054	1.922	1.922	[53]
S-1 and S-2	2.029	1.935	1.915	[36,39]
S3	2.017	2.000	1.968	[39,42]
Rieske	2.01	1.91	1.78	[40,56,57]

iron–sulfur clusters, these can be either paramagnetic (detectable by EPR) or diamagnetic (EPR silent). Many of the electron transfer proteins have been individually characterised before, and their EPR signals, usually consisting of three anisotropic components (Table 1), are known.

We have used the *g*-factors of the iron sulfur clusters, taken from the literature (Table 1), to assign the EPR signals observed in the total EPR spectrum of whole muscle (Fig. 3). In order to obtain the pure lineshapes of individual EPR signals, we tried to use the procedure of spectra deconvolution applied to a set of experimental muscle spectra using a different relative proportion of the individual signals. Unfortunately, this approach proved unsuccessful because the differences in the proportions were not great enough to ensure a good signal-to-noise ratio in the extracted pure lineshape signals. Therefore, we used computer simulations of the pure lineshapes as our basis spectra. Using the published *g*-values as a guide, we slightly changed them in the simulations in order to fit best the peak position in our experimental spectra. We also varied in the simulations the individual line width in order to attain the best correspondence with the experiment (to a first approximation the linewidths were assumed to be isotropic to reduce the number of degrees of freedom in the fitting procedure) The result of the simulation of the four signals from the Fe–S clusters in Complex I is shown in Fig. 5. The intensities of the simulated signals presented in Fig. 5 are the same as the intensities of these signals in the experimental spectrum A. We found these intensities by using the subtraction procedure with variable coefficient, with each simulated signal being subtracted from the experimental spectrum (note Fig. 1).

Spectrum B (Fig. 5) is a result of subtraction of the sum of all four simulated spectra from the experimental spectrum A, i.e., spectrum B does not have any of the signals from the Complex I clusters. The small signal at $g=2.16$ is probably the g_y component of the l.s. form of metMb, with OH^- ion as the 6th coordinating ligand (alkaline Mb) [37], the other two *g*-values at ~2.60 and ~1.83 being below detection level. The signal at $g=2.07$ has not been assigned. However, it should be noted that a similar EPR signal is detected in many biological samples, including purified Hb and Mb preparations [22]. We have previously suggested that this EPR signal can originate from a high spin iron centre with weak bonding and high symmetry [38]. The narrow singlet line with a typical free radical *g*-factor of 2.005 and a linewidth of ~12 G is present in the EPR spectra of many mitochondrial preparations and is usually assigned to the ubisemiquinone radical $SQ^{\bullet}$ [36]. The line marked S3 has a position in the spectrum typical for the oxidised form of iron–sulfur centres S3 in Complex II [39]. It is possible that the first component of the Rieske iron–sulfur centre from Complex III [40] also contributes to this line.

The feature with the *g*-factor of 1.99 in Fig. 5 was also present, though not commented on, in an EPR spectrum from

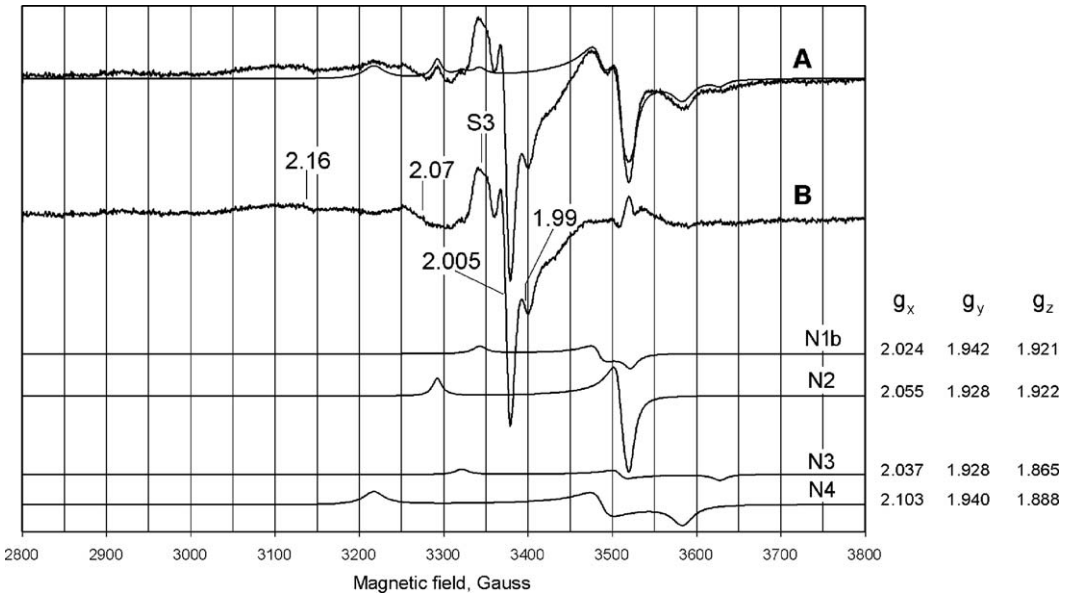

Fig. 5. Illustrative muscle tissue EPR spectrum and simulated EPR signal of the iron–sulfur clusters N1b, N2, N3 and N4 from mitochondrial Complex I. Spectrum A (noisy) is the same as A in Fig. 3; spectrum A (smooth) is a sum of the simulated signals, N1b+N2+N3+N4. The simulated signals are shown with the intensities determined by the procedure of subtraction with variable coefficient (see text). B=A(noisy)−A(smooth). The *g*-values used in the simulations of the N-cluster signals are shown on the right hand side of each simulated EPR signal.

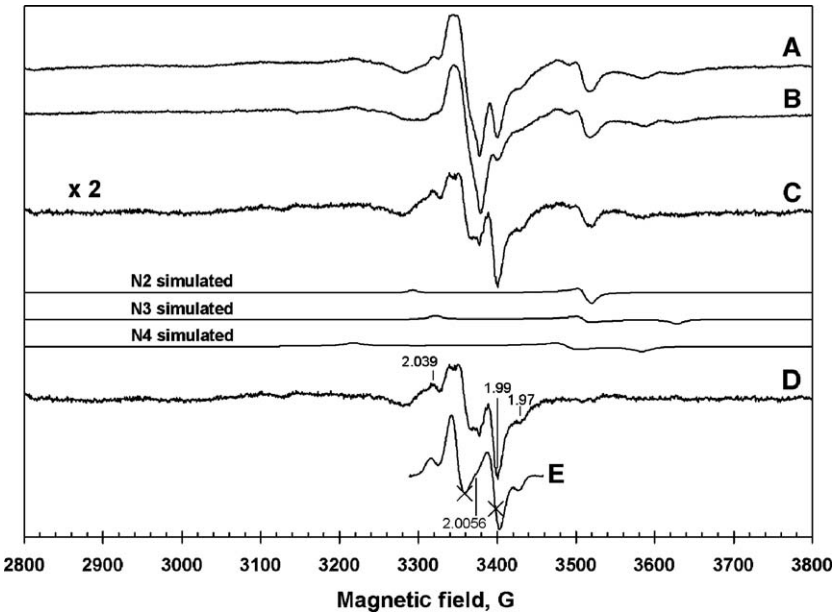

Fig. 6. The use of spectra subtraction with variable coefficient in the extraction of the EPR signal with the $g=1.99$ component. A—an average spectrum of 6 muscle samples from the patients with sepsis, each with a *strong* $g=1.99$ signal; B—an average spectrum of 6 tissue samples from the patients with sepsis, each with a *weak* $g=1.99$ signal; C=2(A−0.72B), the coefficient $k=0.72$ was chosen to minimize the input of all EPR signals non-related to the 1.99 line. D—the same as *C*, but after the simulated signals from N2, N3 and N4 (the same as in Fig. 5) have been subtracted; E— $SQ^{\bullet}$–$SQ^{\bullet}$ pair spectrum as simulated in [43]. The instrumental conditions for spectra A and B were (see Fig. 1 legend for letter coding): $P=13.8$ mW; $\nu=9.468$ GHz, $A_m=3.0$ G; $\nu_m=100$ kHz; $\tau=41$ ms; v=5.96 G/s; $T=10$ K, each of the 6 spectra in both cases was recorded at NS=2. The *g*-factors of main features in spectrum D are indicated. A field scale was attributed to spectrum E simulated in [43] with reference to the two points (marked with crosses) for which the *g*-factors were specified in the original paper (2.0145 and 1.990 [43]) and the values of magnetic field were calculated when ν was allowed to be the same as in spectra A and B, 9.468 GHz. The position of the average *g*-factor of the simulated spectrum E (2.0056) is also indicated.

bovine submitochondrial particles [41]. The 1.99 line is bigger in some muscle samples and smaller in the others. This was used in the extraction of the whole EPR signal (part of which is seen as the 1.99 line) from the overall spectrum (Fig. 6). This figure shows that the whole signal has a quartet-like lineshape.

A similar quartet-like signal with characteristic *g*-factors $g=2.04$, 1.99 and 1.96 has been reported to accompany the signal from S3 centre in mitochondrial membranes [42]. The field position of the components of the signal did not depend on the microwave frequency used; therefore, the multiplicity was assigned to a spin–spin interaction. Since the signal disappeared on depletion of ubiquinone Q, one of the spins was assigned to the ubisemiquinone radical $SQ^{\bullet}$. The other spin was originally thought to originate from S3 (since the S3 and 1.99 go together), but the simulation of the spectrum of the semiquinone–semiquinone pair for a *g*-factor anisotropy of $g_x=2.0041$, $g_y=2.0066$ and $g_z=2.0066$ gave a slightly better fit to the experimental spectrum than the S3–semiquinone system [43]. The possibility of direct spin–spin interaction between ubisemiquinone and S3 has also been criticized [44,45]. Therefore the authors of the study favoured two ubisemiquinone radicals in the radical pair, rather than S3 and an ubisemiquinone radical. However, the ubisemiquinone radical pair is likely to be located in the vicinity of S3 (from the $SQ_s^{\bullet}$ pool), since thenoyltrifluoroacetone (TTFA, a specific inhibitor of the succinate–ubiquinone reductase segment of the respiratory chain) quenched both the ubisemiquinone pair signal and the fraction of the non-coupled (the $g=2.005$ singlet) ubisemiquinone radical that is close to the succinate dehydrogenase $SQ_s^{\bullet}$, in contrast to the fraction of the non-coupled $SQ^{\bullet}$ (the $g=2.005$ singlet) that are close to cytochrome bc_1 ($SQ_c^{\bullet}$) [43].

Following the conclusions made in [43], we suggest that the signal with the 1.99 component in muscle tissue samples originates from a pair of coupled ubisemiquinone radicals, i.e., from an $SQ^{\bullet}$–$SQ^{\bullet}$ radical pair.

We then compared the intensity of all the signals detected as a function of the patients' physiological and chronic health status using a standard intensive care scoring system (APACHE II). This score provides a measure of clinical illness severity and takes into account age, severe chronic comorbidities, core temperature, heart rate, blood pressure, respiratory rate and a range of blood analytes [28]. Higher scores indicate a worse clinical status and an increased likelihood of non-survival. This can be related to the underlying acute illness, such as pneumonia or bowel perforation, to provide a statistical population risk of mortality.

The only component of the EPR detectable species in muscle that showed a significant correlation with the APACHE II score was the radical pair $SQ^{\bullet}$–$SQ^{\bullet}$, where a lower steady state concentration of this species indicated a more severe acute clinical score (Table 2). This again shows the relationship between clinical status in sepsis and muscle mitochondrial bioenergetics [27]. However, we hesitate to interpret this correlation in detail, as little is known about the factors affecting the concentration of this rarely studied species, even in isolated mitochondria. We merely wish to state that the concentration will depend on the redox state of Complex II (note that the redox

Table 2
The slope of the linear regression, correlation coefficient and its confidential interval for different paramagnetic centres in muscle analysed against the APACHE II clinical score (on 23 septic patients)

	Slope	r	95% confidence interval[a]
MetMb	0.018	0.131	(−0.33; 0.54)
Catalase	−0.006	−0.106	(−0.52; 0.35)
Rhombic iron	0.010	0.097	(−0.36; 0.52)
N3	−0.007	−0.097	(−0.53; 0.37)
N4	−0.020	−0.214	(−0.61; 0.27)
N2	−0.020	−0.201	(−0.60; 0.28)
$SQ^{\bullet}$	−0.009	−0.116	(−0.54; 0.36)
S3	−0.014	−0.065	(−0.50; 0.40)
$SQ^{\bullet}$–$SQ^{\bullet}$	−0.039	−0.558	(−0.81; −0.14)

[a] The 95% confidence interval for the correlation coefficient has been determined by using Fisher's transformation of the correlation coefficient r into a normally distributed variable, for which the mean and variance are known, and then inverse Fisher's transformation to express the confidence interval in terms of r. Only in the case of $SQ^{\bullet}$–$SQ^{\bullet}$, the 95% confidence interval does not cover the zero value indicating significance of the non-zero value of the slope.

potentials [43] of the spin-coupled signal are 140 mV for oxidised to semiquinone and 80 mV for semiquinone to fully reduced). Factors that affect Complex II activity (e.g., citric acid cycle flux) might be expected to perturb the steady state concentration of the spin coupled species (arising from an interaction between two radical species this signal would expect to be particularly sensitive to effectors acting to perturb electron flow between them). As we saw no variation in the total Complex II activity in muscle homogenates from patients with severe sepsis [27], an explanation based on irreversible damage/removal of the radical pair is somewhat less attractive than one based on a steady state kinetic argument.

Fig. 7 demonstrates how the lineshape of the muscle tissue EPR spectrum changes when different temperatures are used for EPR measurements. This is caused by the different relaxation characteristics of the paramagnetic centres. The technique of spectra subtraction with variable coefficient, using the pure lineshape signals (Fig. 5) as the subtracted signals, allowed us to measure the intensities of the individual EPR signals in each spectrum presented in the figure and to plot the temperature dependences of the signals (Fig. 7). One might argue that different parts of a signal saturate differently and therefore the spectral subtraction cannot be performed. However, this does not affect the accuracy of our method significantly. Different parts of a signal can saturate differently (whether temperature or power are varied). In practice, however, this effect within the temperature range presented in Fig. 7 manifests itself as variations in the accuracy of the temperature dependencies obtained (see panel at the bottom of Fig. 7). The coincidence of all temperature dependences at the beginning, before saturation starts (0–8 K for all curves or 0–10 K for all but S3, or 0–20 K for SQ and N4), is not perfect, as one might expect from the signals that change their lineshape with temperature. On the other hand the coincidence of the overlapping parts of the curves is good enough for the differences between curves to be less than the variation in a particular species observed in different samples. So we consider it acceptable. It is important to note when comparing *relative* signal between tissue samples, this effect will be irrelevant anyway, unless there is a significant in vivo variation in the saturation properties of the centres.

The signal, that was preliminary assigned to the [3Fe–4S] centre S3 on the basis of its g-factor, is characterised by the fastest decrease of intensity on temperature increase and is not detectable above 20 K. This is a well known characteristics of oxidised centre S3 [46], so the preliminary assignment of the signal to this kind of clusters is confirmed. An alternate explanation is that a signal could arise from oxidatively damaged [3Fe–4S] centres in aconitase (which has similar, though not identical, g-factors to S3). However, unlike S3, the aconitase signal is still detectable up to 25 K [47]. Therefore the complete disappearance of the muscle $g=2.01$ signal at 20 K (Fig. 7) suggests that the vast majority of what we are measuring at 10 K is S3, not aconitase.

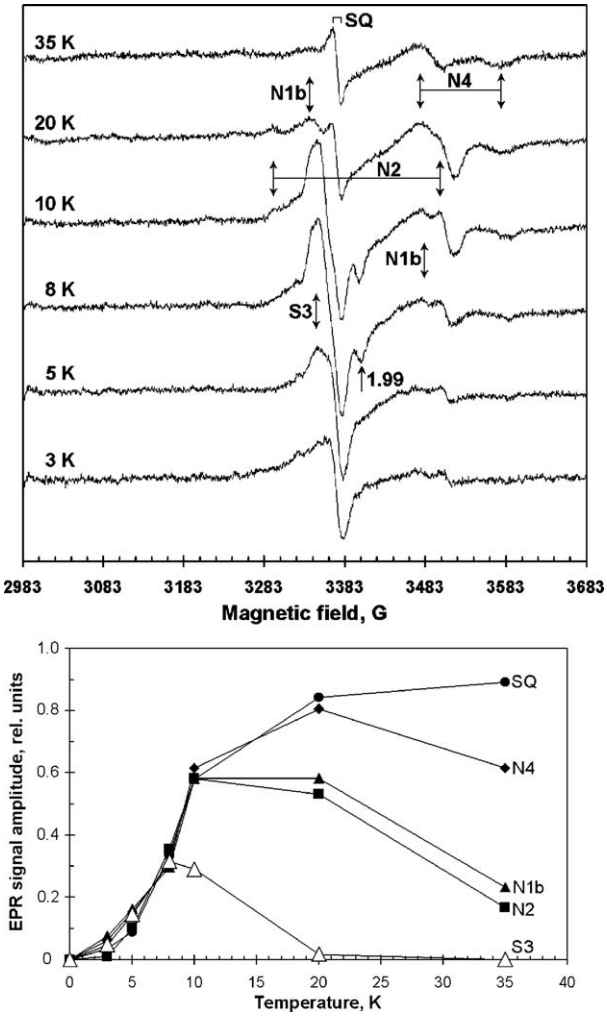

Fig. 7. On top, the EPR spectra of a muscle sample from a septic patient measured at various temperatures (indicated in Kelvin). The components of the identified paramagnetic centres are indicated. Below, the temperature dependences of the identified EPR signals The amplitudes of the signals were measured by the technique of subtraction with variable coefficient, i.e., over the whole line (see Fig. 2) and not at any particular position. All dependences are normalised to a similar course in the temperature interval 0–8 K. The instrumental conditions for the EPR spectra: $P=13.8$ mW; $\nu=9.468$ GHz, $A_m=3.0$ G; $\nu_m=100$ kHz; $\tau=41$ ms; v=16.71 G/s; NS=4.

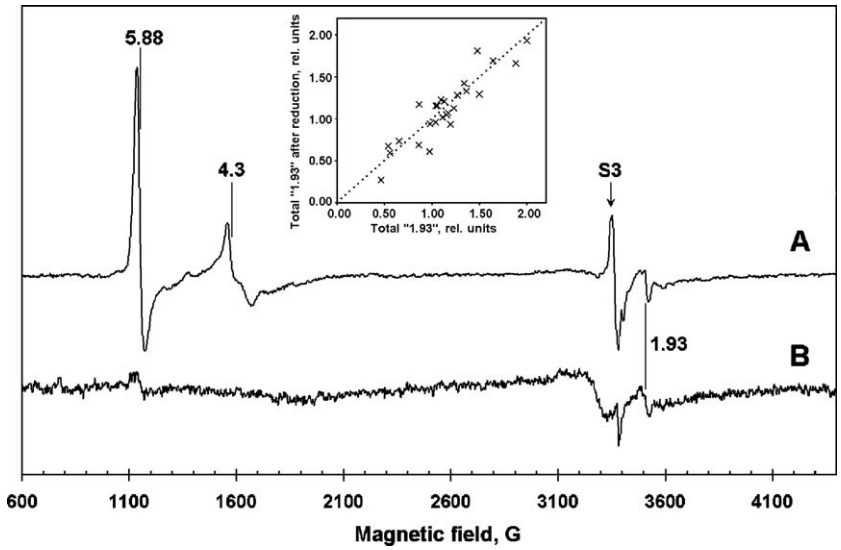

Fig. 8. The EPR spectra of muscle tissue from a septic patient: A, as prepared; B, after the sample was homogenised in 75 mM phosphate buffer (pH 7.4) and reduced with 20 mM dithionite for 3 min at 4 °C. Spectrum B is shown at a 3.87 times greater amplification in accordance with the tissue sample dilution during the reduction. The EPR spectra instrumental conditions: P=3.19 mW; ν=9.469 GHz, A_m=5.0 G; ν_m=100 kHz; τ=82 ms; v=22.64 G/s; NS=1; T=10 K. Inset, the correlation between intensities of the "1.93" signal before and after reduction in 26 samples of muscle tissue. Total "1.93" signal intensity is a measure of the aggregate concentration of the reduced forms of clusters N1b, N3, N4 and N2. Line of identity included for illustrative purposes.

Centre S3 is the only iron–sulfur cluster in the mitochondrial respiratory chain that is paramagnetic in the oxidised form (due to the odd number of iron atoms in the cluster). The presence of the S3 signal in the EPR spectra of muscle tissues means that the chain is not completely reduced. If so, it is possible that there is a population of oxidised (and therefore EPR silent) clusters from Complex I in the tissue, and the measured concentrations of centres N1b, N2, N3 and N4 are underestimated. To explore this possibility, we reduced the tissue samples with dithionite and compared the EPR spectra of the reduced muscle with the spectra of the samples as prepared (Fig. 8). As expected, the reduction resulted in disappearance of the S3 signal, of the h.s. haem signal (g=5.88) and of the rhombic ferric iron signal (g=4.3), all three species being paramagnetic in the oxidised form. The reduction, however, did not result in any appreciable increase of the signal at g=1.93, considered to be an integral measure of the reduced forms of the Complex I clusters. After the reduction procedure the tissue sample is diluted, and its EPR spectrum shows signals of accordingly lower intensity (note that the noise in spectrum B in Fig. 8 becomes greater). The inset in Fig. 8 (data from 26 patient samples) shows that, on average, the intensity of the 1.93 signal does not change on reduction if this

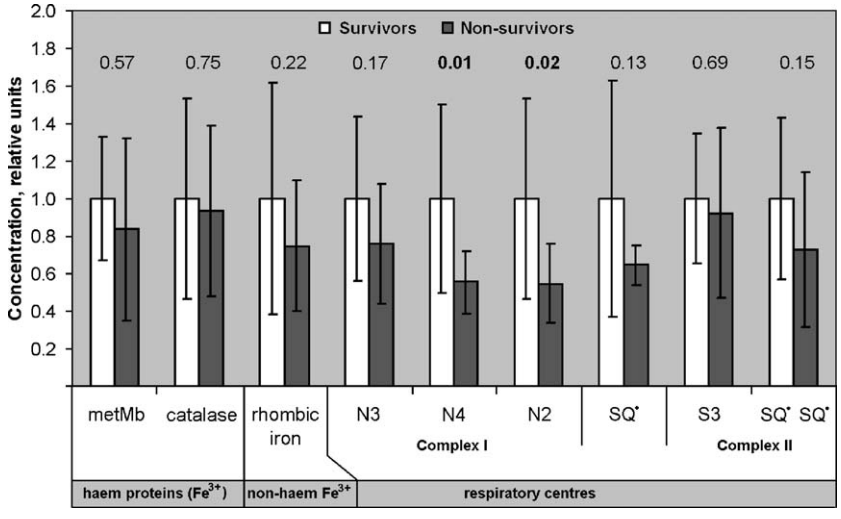

Fig. 9. Relative concentration of different paramagnetic centres in muscle biopsies in two groups of septic patients: in the group of survivors (12 persons) and in those patients who died (11 persons). The centres studied have been classified as follows: haem proteins (catalase and Mb); non-haem Fe^{3+} in a rhombic coordination and the respiratory mitochondrial centres (the iron–sulfur proteins N3, N4 and N2 of the 4Fe–4S type, localised in Complex I; S3 of the 3Fe–4S types, localised in Complex II; ubisemiquinone radicals; ubisemiquinone radical pairs with the g=1.99 component associated with Complex II. The numbers above paired columns indicate the probability associated with the Student's two-tailed heteroscedastic t-test (the probability of the 'survivor' and 'non-survivor' samples being from the same population, i.e., insignificantly different).

dilution factor is taken into account. Therefore, we conclude that Complex I is essentially fully reduced in the muscle tissues as prepared. This is consistent with the data from animal tissue samples frozen in liquid nitrogen [35,48], although human brain samples stored following homogenisation convert predominantly to the oxidised state [49].

3.3. Correlation with clinical outcome

We can now use this method to study the relative concentration of different paramagnetic centres in vivo. In this case we ignore cluster N1b since its EPR signal intensity, being the lowest among the Complex I centres, cannot be accurately determined. Additionally, its spectrum is similar to that of S1, the reduced [2Fe–2S] centre in complex II, and, although we do not think that we detect reduced S1 in the muscle samples, we are not totally confident that changes in its concentration would not contaminate the deconvolution process.

Fig. 9 shows the relative concentration of different paramagnetic centres in muscle in the patients suffering from severe sepsis, grouped as to whether they survived or not. We have previously shown a significant fall in muscle ATP levels measured at day 1 for those patients who subsequently die [27]. There is also a tendency for isolated Complex I activity in muscle homogenates to be lower in the non-survivors. While the random error in the determination of the paramagnetic components in muscle is relatively high, we see a statistically significant decrease in the intensity of centres N4 and N2 in the non-survivors. Both these centres are located in Complex I (Fig. 4) and this confirms the trend that we saw in the isolated enzyme activities.

The lower concentration of N4 and N2 in the non-survivors can be explained in a number of ways. First, the electron transfer chain could be inhibited, such that there is decreased reduction of these centres that is maintained during the freezing process, e.g., by an inhibitory block between N3 and N4. We do not favour this explanation as the dithionite experiments suggest the Complex I iron–sulfur clusters in the chain are essentially fully reduced in all the samples. Inhibition of electron flux also might be expected to affect the S3 redox state, which does not happen. An alternative possibility is that N2 and N4 are specifically damaged, i.e., there are Complex I species lacking these centres. In favour of this is the fact that another Complex I centre, N3 is not significantly different between the two groups. While we cannot rule this out, we consider it an over-interpretation of the N3 data. There is a tendency for N3 to be lower in the non-survivors and it has a large random error. Therefore, we favour the third, simplest explanation of the data, i.e., that patients in the non-survivor group have, on average, less Complex I molecules per mitochondria than those that survive. In principle, quantitative immunoassays or proteomic techniques could be used to support the contention that the reduced Complex I activity and decrease in detectable EPR species in muscle homogenates is merely a consequence of a decreased enzyme content; however, the relatively small changes detected here might be difficult to confirm.

This analysis is consistent with the trend from our previous studies [27] and from long-term animal models of sepsis [50]. It confirms that mitochondrial dysfunction (and particularly Complex I damage) is linked to the aetiology of septic shock. We have not shown a causal nature of this link; however, we do note increased nitric oxide and decreased glutathione levels in muscle biopsies from these patients [27]. Complex I is particularly susceptible to irreversible damage by NO and peroxynitrite, especially when glutathione levels are low [51]. Furthermore, perturbations in electron flow at the level of Complex I may have more far-reaching effects than a simple decrease in respiratory flux, given that it is a major source of mitochondrial free radical production [52].

4. Conclusion

EPR spectroscopy can be used to describe both qualitatively and quantitatively the paramagnetic status of a complex system containing many paramagnetic centres. By using the techniques of spectra subtraction with variable coefficient, it is possible to follow changes in the concentrations of individual centres. While *absolute* concentrations might be relatively error prone, *relative* changes in the concentration of individual centres in similar experimental systems are likely to be more robust. The data presented on muscle biopsies clearly illustrate the usefulness of this approach in a complex real world situation.

Acknowledgement

This work has been supported by the Wellcome Trust.

References

[1] D.A. Svistunenko, R.P. Patel, S.V. Voloshchenko, M.T. Wilson, The globin-based free radical of ferryl hemoglobin is detected in normal human blood, J. Biol. Chem. 272 (1997) 7114–7121.
[2] D.A. Svistunenko, N.A. Davies, M.T. Wilson, R.P. Stidwill, M. Singer, C. E. Cooper, Free radical in blood: a measure of haemoglobin autoxidation in vivo? J. Chem. Soc., Perkin Trans. 2 (1997) 2539–2543.
[3] D.A. Svistunenko, J. Dunne, M. Fryer, P. Nicholls, B.J. Reeder, M.T. Wilson, M.G. Bigotti, F. Cutruzzola, C.E. Cooper, Comparative study of tyrosine radicals in hemoglobin and myoglobins treated with hydrogen peroxide, Biophys. J. 83 (2002) 2845–2855.
[4] T. Ohnishi, Mitochondrial iron–sulfur flavodehydrogenases, Membrane Proteins in Energy Transduction, Marcel Dekker, New York, 1979, pp. 1–87.
[5] H. Beinert, S.P. Albracht, New insights, ideas and unanswered questions concerning iron–sulfur clusters in mitochondria, Biochim. Biophys. Acta 683 (1982) 245–277.
[6] B. Commoner, J.L. Ternberg, Free radicals in surviving tissues, Proc. Natl. Acad. Sci. U. S. A. 47 (1961) 1374–1384.
[7] E.K. Ruuge, I.A. Kornienko, EPR spectra of frozen animal tissues [in Russ], Biofizika 14 (1969) 752–754.
[8] D.L. Williams-Smith, P.J. Morrison, Electron paramagnetic resonance spectra of catalase in mammalian tissues, Biochim. Biophys. Acta 405 (1975) 253–261.
[9] D.S. Burbaev, A.F. Vanin, N.V. Voevodskaia, A.V. Lebanidze, EPR spectra of animal tissues in vitro [in Russ], Biofizika 20 (1975) 1062–1067.
[10] N.V. Voevodskaia, D.S. Burbaev, A.F. Vanin, L.A. Blumenfeld, EPR study of flavo- and ubisemiquinones in liver tissue [in Russ], Mol. Biol. (Moskva) 15 (1981) 243–251.
[11] M.K. Pulatova, D.E. Filatov, V.L. Sharygin, L.B. Gorbacheva, K.V. Gudtsova, Z.V. Kuropteva, T.T. Zhumabaeva, V.I. Shamaev, D.B. Korman, The EPR spectra of the ribonucleotide reductase in the tumorous tissues and organs of tumor-bearing animals, Izv. Akad. Nauk SSSR, Biol. (1990) 737–748.

[12] D.A. Svistunenko, Ascorbic acid radicals induced by the action of radiation in tissues from rat organs frozen at 77 K, Izv. Akad. Nauk SSSR, Biol. (1990) 827–834.
[13] E.K. Ruuge, A.N. Ledenev, V.L. Lakomkin, A.A. Konstantinov, M. Ksenzenko, Free radical metabolites in myocardium during ischemia and reperfusion, Am. J. Physiol. 261 (1991) 81–86.
[14] S. Premaratne, W. Limm, M.M. Mugiishi, L.H. Piette, J.J. McNamara, Quantitative assessment of free-radical generation during ischemia and reperfusion in the isolated rabbit heart, Coron. Artery Dis. 4 (1993) 1093–1096.
[15] D.P. Naughton, M.C. Symons, When is a radical not a radical? Free Radic. Res. 25 (1996) 1–3.
[16] L. Zecca, H.M. Swartz, Total and paramagnetic metals in human substantia nigra and its neuromelanin, J. Neural Transm., Parkinson's Dis. Dement. Sect. 5 (1993) 203–3213.
[17] H.M. Swartz, K.J. Liu, F. Goda, T. Walczak, India ink: a potential clinically applicable EPR oximetry probe, Magn. Reson. Med. 31 (1994) 229–232.
[18] S.L. Breen, J.J. Battista, Radiation dosimetry in human bone using electron paramagnetic resonance, Phys. Med. Biol. 40 (1995) 2065–2077.
[19] N.V. Gorbunov, Y.Y. Tyurina, G. Salama, B.W. Day, H.G. Claycamp, G. Argyros, N.M. Elsayed, V.E. Kagan, Nitric oxide protects cardiomyocytes against tert-butyl hydroperoxide-induced formation of alkoxyl and peroxyl radicals and peroxidation of phosphatidylserine, Biochem. Biophys. Res. Commun. 244 (1998) 647–651.
[20] M. Sok, M. Sentjurc, M. Schara, Membrane fluidity characteristics of human lung cancer, Cancer Lett. 139 (1999) 215–220.
[21] D.A. Svistunenko, M.A. Sharpe, P. Nicholls, M.T. Wilson, C.E. Cooper, A new method for quantitation of spin concentration by EPR spectroscopy: application to methemoglobin and metmyoglobin, J. Magn. Reson. 142 (2000) 266–275.
[22] D.A. Svistunenko, M.A. Sharpe, P. Nicholls, C. Blenkinsop, N.A. Davies, J. Dunne, M.T. Wilson, C.E. Cooper, The pH dependence of naturally occurring low-spin forms of methaemoglobin and metmyoglobin: an EPR study, Biochem. J. 351 (2000) 595–605.
[23] D.A. Svistunenko, An EPR study of the peroxyl radicals induced by hydrogen peroxide in the haem proteins, Biochim. Biophys. Acta 1546 (2001) 365–378.
[24] J.P. McHugh, F. Rodriguez-Quinones, H. Abdul-Tehrani, D.A. Svistunenko, R.K. Poole, C.E. Cooper, S.C. Andrews, Global iron-dependent gene regulation in *Escherichia coli*. A new mechanism for iron homeostasis, J. Biol. Chem. 278 (2003) 29478–29486.
[25] A.F. Vanin, D.A. Svistunenko, V.D. Mikoyan, V.A. Serezhenkov, M.J. Fryer, N.R. Baker, C.E. Cooper, Endogenous superoxide production and the nitrite/nitrate ratio control the concentration of bioavailable free nitric oxide in leaves, J. Biol. Chem. 279 (2004) 24100–24107.
[26] S.A. Malone, A. Lewin, M.A. Kilic, D.A. Svistunenko, C.E. Cooper, M.T. Wilson, N.E. Le Brun, S. Spiro, G.R. Moore, Protein-template-driven formation of polynuclear iron species, J. Am. Chem. Soc. 126 (2004) 496–504.
[27] D. Brealey, M. Brand, I. Hargreaves, S. Heales, J. Land, R. Smolenski, N. A. Davies, C.E. Cooper, M. Singer, Association between mitochondrial dysfunction and severity and outcome of septic shock, Lancet 360 (2002) 219–223.
[28] W.A. Knaus, E.A. Draper, D.P. Wagner, J.E. Zimmerman, APACHE II: a severity of disease classification system, Crit. Care Med. 13 (1985) 818–829.
[29] J. Peisach, W.E. Blumberg, S. Ogawa, E.A. Rachmilewitz, R. Oltzik, The effect of protein conformation on the heme symmetry in high spin ferric heme proteins as studied by electron paramagnetic resonance, J. Biol. Chem. 246 (1971) 3342–3355.
[30] W.E. Blumberg, J. Peisach, A unified theory for low spin forms of all ferric heme proteins as studied by EPR, in: B. Chance, T. Yonetani, A.S. Mildvan (Eds.), Probes of structure and function of macromolecules and membranes, Academic Press, New York, 1971, pp. 215–229.
[31] J. Peisach, W.E. Blumberg, E.T. Lode, M.J. Coon, An analysis of the electron paramagnetic resonance spectrum of *Pseudomonas oleovorans* rubredoxin. A method for determination of the ligands of ferric iron in completely rhombic sites, J. Biol. Chem. 246 (1971) 5877–5881.
[32] P. Aisen, R. Aasa, B.G. Malmstrom, T. Vanngard, Bicarbonate and the binding of iron to transferrin, J. Biol. Chem. 242 (1967) 2484–2490.
[33] E.I. Solomon, Bioinorganic perspectives in copper coordination chemistry, in: K.D. Karlin, J. Zubieta (Eds.), Copper coordination chemistry : biochemical and inorganic perspectives, Adenine Press, Guilderland (NY), 1983, pp. 1–22.
[34] L. Calabrese, M. Carbonaro, G. Musci, Chicken ceruloplasmin. Evidence in support of a trinuclear cluster involving type 2 and 3 copper centers, J. Biol. Chem. 263 (1988) 6480–6483.
[35] R. Cammack, C.E. Cooper, Electron paramagnetic resonance spectroscopy of iron complexes and iron-containing proteins, Methods Enzymol. 227 (1993) 353–384.
[36] T. Ohnishi, Iron–sulfur clusters/semiquinones in complex I, Biochim. Biophys. Acta 1364 (1998) 186–206.
[37] J.A. Berzofsky, J. Peisach, W.E. Blumberg, Sulfheme proteins: I. Optical and magnetic properties of sulfmyoglobin and its derivatives, J. Biol. Chem. 246 (1971) 3367–3377.
[38] D.A. Svistunenko, A. Rob, A. Ball, J. Torres, M.C. Symons, M.T. Wilson, C.E. Cooper, The electron paramagnetic resonance characterisation of a copper- containing extracellular peroxidase from *Thermomonospora fusca* BD25, Biochim. Biophys. Acta 1434 (1999) 74–85.
[39] S. Anemüller, T. Hettmann, R. Moll, M. Teixeira, G. Schäfer, EPR characterization of an archaeal succinate dehydrogenase in the membrane-bound state, Eur. J. Biochem. 232 (1995) 563–568.
[40] W. Schlenzka, L. Shaw, S. Kelm, C.L. Schmidt, E. Bill, A.X. Trautwein, F. Lottspeich, R. Schauer, CMP-N-acetylneuraminic acid hydroxylase: the first cytosolic Rieske iron–sulphur protein to be described in Eukarya, FEBS Lett. 385 (1996) 197–200.
[41] T. Ohnishi, V.D. Sled, T. Yano, T. Yagi, D.S. Burbaev, A.D. Vinogradov, Structure–function studies of iron–sulfur clusters and semiquinones in the NADH-Q oxidoreductase segment of the respiratory chain, Biochim. Biophys. Acta 1365 (1998) 301–308.
[42] F.J. Ruzicka, H. Beinert, K.L. Schepler, W.R. Dunham, R.H. Sands, Interaction of ubisemiquinone with a paramagnetic component in heart tissue, Proc. Natl. Acad. Sci. U. S. A. 72 (1975) 2886–2890.
[43] J.C. Salerno, Ohnishi, T. Studies on the stabilized ubisemiquinone species in the succinate–cytochrome *c* reductase segment of the intact mitochondrial membrane system, Biochem. J. 192 (1980) 769–781.
[44] W.J. Ingledew, T. Ohnishi, Properties of the S-3 iron–sulphur centre of succinate dehydrogenase in the intact respiratory chain of beef heart mitochondria, FEBS Lett. 54 (1975) 167–171.
[45] W.J. Ingledew, J.C. Salerno, T. Ohnishi, Studies on electron paramagnetic resonance spectra manifested by a respiratory chain hydrogen carrier, Arch. Biochem. Biophys. 177 (1976) 176–184.
[46] M.K. Johnson, J.E. Morningstar, D.E. Bennett, B.A. Ackrell, E.B. Kearney, Magnetic circular dichroism studies of succinate dehydrogenase. Evidence for [2Fe–2S], [3Fe–xS], and [4Fe–4S] centers in reconstitutively active enzyme, J. Biol. Chem. 260 (1985) 7368–7378.
[47] J.K. Shergill, R. Cammack, J.H. Chen, M.J. Fisher, S. Madden, H.H. Rees, EPR spectroscopic characterization of the iron–sulphur proteins and cytochrome *P*-450 in mitochondria from the insect *Spodoptera littoralis* (cotton leafworm), Biochem. J. 307 (1995) 719–728.
[48] D.S. Burbaev, A.F. Vanin, A.I. Sergeev, I.P. Solojhenkin, N.V. Volkova, E.I. Galperin, The increase of oxidation level in the iron–sulphur proteins from the isolated tissues of mammals and patients under some pathologies, Stud. Biophys. 99 (1984) 143–150.
[49] J.K. Shergill, R. Cammack, C.E. Cooper, J.M. Cooper, V.M. Mann, A.H. Schapira, Detection of nitrosyl complexes in human substantia nigra, in relation to Parkinson's disease, Biochem. Biophys. Res. Commun. 228 (1996) 298–305.
[50] D. Brealey, S. Karyampudi, T.S. Jacques, M. Novelli, R. Stidwill, V. Taylor, R.T. Smolenski, M. Singer, Mitochondrial dysfunction in a long-term rodent model of sepsis and organ failure, Am. J. Physiol., Regul. Integr. Comp. Physiol. 286 (2004) R491–R497.
[51] J.P. Bolanos, A. Almeida, V. Stewart, S. Peuchen, J.M. Land, J.B. Clark, S.J. Heales, Nitric oxide-mediated mitochondrial damage in the brain: mechanisms and implications for neurodegenerative diseases, J. Neurochem. 68 (1997) 2227–2240.
[52] A.J. Lambert, M.D. Brand, Inhibitors of the quinone-binding site allow rapid superoxide production from mitochondrial NADH:ubiquinone oxidoreductase (complex I), J. Biol. Chem. 279 (2004) 39414–39420.

[53] H. Beinert, R.H. Sands, Biochem. Biophys. Res. Commun. 3 (1960) 41–45.
[54] T. Ohnishi, Thermodynamic and EPR characterization of iron–sulfur centers in the NADH–ubiquinone segment of the mitochondrial respiratory chain in pigeon heart, Biochim. Biophys. Acta 387 (1975) 475–490.
[55] S.P. Albracht, G. Dooijewaard, F.J. Leeuwerik, B.V. Swol, EPR signals of NADH: Q oxidoreductase. Shape and intensity, Biochim. Biophys. Acta 459 (1977) 300–317.
[56] R.C. Prince, J.G. Lindsay, P.L. Dutton, The Rieske iron–sulfur center in mitochondrial and photosynthetic systems: Em/pH relationships, FEBS Lett. 51 (1975) 108–111.
[57] E. Davidson, T. Ohnishi, E. Atta-Asafo-Adjei, F. Daldal, Potential ligands to the [2Fe–2S] Rieske cluster of the cytochrome bc1 complex of *Rhodobacter capsulatus* probed by site-directed mutagenesis, Biochemistry 31 (1992) 3342–3351.